

RESEARCH

Open Access



PSAT1 positively regulates the osteogenic lineage differentiation of periodontal ligament stem cells through the ATF4/*PSAT1*/Akt/GSK3 β / β -catenin axis

Linglu Jia^{1,3,4,5}, Dongfang Li^{3,4,5}, Ya-Nan Wang^{2,3,4,5}, Dongjiao Zhang^{2,3,4,5*} and Xin Xu^{2,3,4,5*} 

Abstract

Background Periodontal ligament stem cells (PDLSCs) are important seed cells for tissue engineering to realize the regeneration of alveolar bone. Understanding the gene regulatory mechanisms of osteogenic lineage differentiation in PDLSCs will facilitate PDLSC-based bone regeneration. However, these regulatory molecular signals have not been clarified.

Methods To screen potential regulators of osteogenic differentiation, the gene expression profiles of undifferentiated and osteodifferentiated PDLSCs were compared by microarray and bioinformatics methods, and *PSAT1* was speculated to be involved in the gene regulation network of osteogenesis in PDLSCs. Lentiviral vectors were used to overexpress or knock down *PSAT1* in PDLSCs, and then the proliferation activity, migration ability, and osteogenic differentiation ability of PDLSCs in vitro were analysed. A rat mandibular defect model was built to analyse the regulatory effects of *PSAT1* on PDLSC-mediated bone regeneration in vivo. The regulation of *PSAT1* on the Akt/GSK3 β / β -catenin signalling axis was analysed using the Akt phosphorylation inhibitor Ly294002 or agonist SC79. The potential sites on the promoter of *PSAT1* that could bind to the transcription factor ATF4 were predicted and verified.

Results The microarray assay showed that the expression levels of 499 genes in PDLSCs were altered significantly after osteogenic induction. Among these genes, the transcription level of *PSAT1* in osteodifferentiated PDLSCs was much lower than that in undifferentiated PDLSCs. Overexpressing *PSAT1* not only enhanced the proliferation and osteogenic differentiation abilities of PDLSCs in vitro, but also promoted PDLSC-based alveolar bone regeneration in vivo, while knocking down *PSAT1* had the opposite effects in PDLSCs. Mechanistic experiments suggested that *PSAT1* regulated the osteogenic lineage fate of PDLSCs through the Akt/GSK3 β / β -catenin signalling axis. *PSAT1* expression in PDLSCs during osteogenic differentiation was controlled by transcription factor ATF4, which is realized by the combination of ATF4 and the *PSAT1* promoter.

Conclusion *PSAT1* is a potential important regulator of the osteogenic lineage differentiation of PDLSCs through the ATF4/*PSAT1*/Akt/GSK3 β / β -catenin signalling pathway. *PSAT1* could be a candidate gene modification target for enhancing PDLSCs-based bone regeneration.

*Correspondence:

Dongjiao Zhang
djzhang1109@163.com
Xin Xu
xinxu@sdu.edu.cn

Full list of author information is available at the end of the article



© The Author(s) 2023. **Open Access** This article is licensed under a Creative Commons Attribution 4.0 International License, which permits use, sharing, adaptation, distribution and reproduction in any medium or format, as long as you give appropriate credit to the original author(s) and the source, provide a link to the Creative Commons licence, and indicate if changes were made. The images or other third party material in this article are included in the article's Creative Commons licence, unless indicated otherwise in a credit line to the material. If material is not included in the article's Creative Commons licence and your intended use is not permitted by statutory regulation or exceeds the permitted use, you will need to obtain permission directly from the copyright holder. To view a copy of this licence, visit <http://creativecommons.org/licenses/by/4.0/>. The Creative Commons Public Domain Dedication waiver (<http://creativecommons.org/publicdomain/zero/1.0/>) applies to the data made available in this article, unless otherwise stated in a credit line to the data.

Keywords PSAT1, Periodontal ligament stem cells, Osteogenic differentiation, Microarray assay

Introduction

Periodontal disease, trauma, tumours, etc. can cause the destruction and loss of alveolar bones, damaging the physiological function of people. Rapidly developing bone tissue engineering has become an attractive approach to achieve the regeneration of defective bones [1, 2]. Seed cells, scaffolds and growth factors, which are the main component elements of bone tissue engineering, have been widely studied and show beneficial effects on bone regeneration [3].

Periodontal ligament stem cells (PDLSCs), a type of adult mesenchymal stem cell (MSC), have received increasing attention as seed cells for bone tissue engineering, because they have considerable capabilities in proliferation, osteogenic lineage differentiation and anti-apoptosis [4–7]. In addition, the tissue sources of PDLSCs are rich and minimally invasive, because they can be obtained from extracted third molars [5]. Several studies have proven that the use of culture-expanded PDLSCs with various biomaterials or growth factors promoted the regeneration of defective maxillo-facial bone to a certain degree in animal models [8–11]. However, there is still a gap between the effects of tissue engineering and clinical expectations.

Elaborating the molecular mechanisms underlying the osteogenic differentiation of PDLSCs will help to explore methods to enhance PDLSC-based bone regeneration. To date, a large number of genes and proteins, and the signalling pathways in which they participate have been proven to affect the osteogenic differentiation of PDLSCs, including RUNX2 [12], Wnt/ β -catenin signalling pathway-related proteins [13], PI3K/Akt signalling pathway-related proteins [14], MAPK signalling pathway-related proteins [15], etc. However, the exact inner regulatory networks that underlie the osteogenic lineage fate of PDLSCs remain unclear. To search for potential important regulators of osteogenic differentiation, the present study filtered differentially expressed coding-genes between undifferentiated and osteodifferentiated PDLSCs by microarray assay, and conducted a primary analysis through bioinformatics methods. Notably, *PSAT1*, the expression of which was altered significantly during the osteogenic differentiation of PDLSCs, seemed to be a potential regulator.

Phosphoserine aminotransferase 1 (PSAT1), encoded by the gene *PSAT1*, is a type of protein with enzyme activity that participates in L-serine metabolism [16]. *PSAT1* is widely expressed in tissue cells and has been proven to affect a variety of physiological functions. For

example, hepatic *Psat1* was demonstrated to regulate insulin sensitivity in mice [17]. *PSAT1* was reported to be required for collagen protein production by lung fibroblasts in humans [18]. Mutations in the *PSAT1* gene lead to the development of some mental diseases and congenital developmental abnormalities [19–22]. In addition, *PSAT1* was reported to be overexpressed in some types of tumours and could affect the proliferation or invasion of cancer cells, including esophageal squamous cell carcinoma, colon cancer, and non-small cell lung cancer cells [23–27]. It is worth noting that a recent study proved that *Psat1* affected the timing of mouse embryonic stem cell (ESC) differentiation in a serine-independent manner [28]. Another study revealed a connection between *Psat1* expression and extracellular matrix mineralization in mouse osteoblasts [29]. In addition, the serine metabolic pathway that *PSAT1* involved in was reported to affect the ageing of dental pulp stem cells [30]. Based on the above facts and the results of the microarray assay, we speculated that *PSAT1* may play a regulatory role in the osteogenic differentiation of PDLSCs and aimed to investigate this possibility.

In this study, we provided evidence of the regulatory effects of *PSAT1* on PDLSC osteogenic differentiation in vivo and in vitro. In addition, we revealed that *PSAT1* affected the osteogenesis of PDLSCs through the Akt/GSK3 β / β -catenin signalling pathway. Furthermore, *PSAT1* expression was regulated by the transcription factor ATF4 during the osteogenic differentiation of PDLSCs. We hope that these results provide new ideas for the study of gene regulatory networks of osteogenic lineage differentiation in PDLSCs.

Materials and methods

Cell isolation and cultivation

Healthy premolars that were extracted due to orthodontic treatment were collected. The donors were aged from 16 to 24 years-old and were systemically healthy. The periodontal ligament tissues were scraped from the middle third of the root surface and minced. Then, the tissues were attached to the bottom of the culture flask and incubated for 2 h at 37 °C in a 5% CO₂ incubator. Finally, the complete culture medium containing alpha-minimal essential medium (α -MEM) (BI, Beit Haemek, Israel) and 10% foetal bovine serum (FBS) (BI) was added to the culture flask. The medium was refreshed every 3 days after the cells grew out of the tissue masses. Cells were passaged using trypsin/EDTA (Solarbio, Beijing, China) after

reaching 90% confluence, and cells at passages 3–6 were used for the experiments.

Immuno-phenotype assay

To analyse the immune-phenotype of PDLSCs, the BD Human MSC Analysis Kit (BD Biosciences, NJ, USA) was used according to the manufacturer's instructions. In brief, cells were harvested and incubated with antibodies conjugated with fluorescent dyes in the dark at 4 °C for 30 min. Then, the cells were washed with phosphate-buffered saline (PBS) and detected by flow cytometry. Antibodies of the kit included MSC-positive markers (CD90, CD105, CD73, CD44) and MSC-negative markers (CD34, CD11, CD19, CD45, HLA-DR).

Clonogenic assay

PDLSCs were seeded into 6-well culture plates at a density of 200 cells per well and cultured in complete culture medium for 10 days. Then, the cells were fixed with paraformaldehyde and stained with 0.1% crystal violet (Solarbio). Finally, the cells were observed under the microscope, and aggregates with more than 50 cells were regarded as clones.

Multilineage differentiation assay

For the osteogenic differentiation assay, PDLSCs were cultured in osteogenic medium containing α -MEM (BI), 10% FBS (BI), 10 nM dexamethasone (Solarbio), 10 mM β -glycerophosphate (Solarbio) and 50 mg/L ascorbic acid (Solarbio). After 4 weeks, the cells were fixed with paraformaldehyde and stained with Alizarin Red solution (Sigma, St. Louis, MO, USA) to detect mineralized nodules. To analyse the intensity of Alizarin red staining, mineralized nodules were dissolved in 10% cetylpyridinium chloride (Solarbio) and quantified using a microplate reader at 562 nm. When necessary, Ly294002 (#9901, CST) (an inhibitor of Akt phosphorylation) or SC79 (HY-18749, MCE, USA) (a promoter of Akt phosphorylation) was added to the osteogenic medium at concentration of 10 μ mol/L or 5 μ g/mL, respectively.

For the adipogenic differentiation assay, PDLSCs were cultured in adipogenic medium containing α -MEM (BI), 10% FBS (BI), 1 μ M dexamethasone (Solarbio), 0.2 mM indomethacin (Solarbio), 0.01 g/L insulin (Solarbio) and 0.5 mM isobutyl-methylxanthine (Solarbio). Four weeks later, the cells were fixed with paraformaldehyde and stained with oil red O (Solarbio) to detect lipid droplets.

Microarray analyses and bioinformatics analyses

Three PDLSC clones obtained from three different individuals were cultured in osteogenic medium for 7 days (OI PDLSCs), and the corresponding PDLSCs cultured in complete culture medium for 7 days were regarded as

the control (NC PDLSCs). Then, the cells were collected for microarray analyses through GeneChip Human Transcriptome Array 2.0 (Affymetrix, USA) according to the manufacturer's instructions with the help of a company (GMINIX Informatics Ltd., Co., Shanghai, China). The differentially expressed genes between OI PDLSCs and NC PDLSCs were filtered using the significance analysis of microarrays (SAM) method [31]. Fold change (FC), which reflected the change in gene expression level, was calculated, and its absolute value represented the change range, and the positive or negative sign represented upregulation or downregulation.

The differentially expressed genes were further analysed through GO analyses and pathway analyses. GO analyses were based on the Gene Ontology Consortium database, which identified the function of genes in terms of biological process (BP), cellular component (CC) and molecular function (MF). Pathway analyses were based on the Kyoto Encyclopedia of Genes and Genomes (KEGG) database, which confirmed which biological pathways these differentially expressed genes participated in. Furthermore, hybrid hierarchical clustering algorithm was used to analyse the relationships among differentially expressed genes, and the correlation coefficient of each pair was calculated.

Cell proliferation assay

The cell counting Kit-8 kit (CCK-8) (Dojindo Laboratories, Kumamoto, Japan) and EdU detection kit (RiboBio, Guangzhou, China) were used to analyse cell proliferation according to the manufacturer's instructions. For the CCK-8 assay, cells were incubated in complete culture medium containing 10% CCK-8 solution at 37 °C for 2 h, and then the absorbance at 450 nm was measured by a microplate reader. For the EdU assay, cells were incubated in 50 μ M EdU labelling medium at 37 °C for 2 h, and then fixed and stained with Apollo[®] 567 solution and Hoechst 33342 solution. Afterwards, the cells were observed under a fluorescence microscope and photographed. The percentage of EdU-positive cells among the total cells was calculated based on 6 random fields.

Cell cycle assay

To detect the cell cycle distribution of cells, a cell cycle and apoptosis analysis kit (Beyotime, Shanghai, China) was used according to the manufacturer's instructions, and then the cells were analysed by flow cytometry.

ALP staining and quantitative analysis of ALP activity

To measure the activity of alkaline phosphatase (ALP), ALP staining and quantitative analysis of ALP activity were used. For ALP staining, PDLSCs were stained using the NBT/BCIP staining kit (Beyotime) according to

the manufacturer's instructions, and then the cells were observed under microscope. For the quantitative analysis of ALP activity, PDLSCs were lysed and assayed using an ALP assay kit (Nanjing Jiancheng Bioengineering Institute, Nanjing, China).

Cell migration assay

Cells were plated in a culture dish with complete culture medium. At 90% confluency, a vertical line was scratched in the culture dish using a sterile pipette tip, and the exfoliated cells were washed off by PBS. The cells in the culture dish were incubated in α -MEM (BI) supplemented with 0.5% FBS (BI), and images at the 0th hour, 24th hour, and 36th hour were captured under a microscope. Finally, ImageJ software was used to analyse the migration areas.

Small interfering RNA (siRNA) and plasmid transfection

siRNAs were designed and synthesized by GenePharma Corporation (Shanghai, China) to downregulate the expression of target genes, and siRNA-targeted none was used as the control (siNC group). The siRNA primers are shown in Additional file 1. To overexpress *ATF4*, the pcDNA3.1 vector containing full-length *ATF4* was used (OE *ATF4* group), and the empty pcDNA3.1 vector was used as the control (pcDNA3.1 group). Transfection of PDLSCs with siRNAs and plasmids was performed using Micropoly-transfecter cell reagent (Micropoly, Jiangsu, China) according to the manufacturer's protocol.

Lentivirus transfection

To overexpress or knockdown *PSAT1* in PDLSCs, the *PSAT1*-overexpression vector (pGLV3H1-GFP-puro) and the short hairpin RNA (shRNA) duplex oligo targeting *PSAT1* (pEF-1 α F-GFP-puro) were packaged into lentiviruses (Genechem, Shanghai, China). The pGLV3H1-GFP-puro empty vector and nontargeting shRNA pEF-1 α F-GFP-puro were also packaged into lentiviruses as a control. PDLSCs were incubated in complete culture medium supplemented with lentiviruses and polybrene (Genechem) for 6 h, and then incubated in complete culture medium supplemented with puromycin (Solarbio) for 1 week. Finally, PDLSCs with *PSAT1* overexpression (OE*PSAT1*), PDLSCs with *PSAT1* knockdown (sh*PSAT1*), and their respective control groups (OENC, shNC) were obtained.

Protein extraction and Western Blot

The total proteins of cells were extracted using RIPA buffer (Solarbio) containing protease inhibitor (Solarbio) and phosphatase inhibitor (Bosterbio, Wuhan, China). The cytoplasmic and nuclear proteins of cells were extracted using the Nuclear and Cytoplasmic Protein Extraction Kit (Bosterbio). The proteins were separated

by SDS-PAGE and transferred to polyvinylidene difluoride membranes. Then, the membranes were blocked with nonfat milk and incubated with primary antibodies overnight at 4 °C, followed by incubation with secondary antibodies conjugated with horseradish peroxidase. Finally, the signals on the membranes were detected by enhanced chemiluminescence reagent under an Amersham Imager 600 (General Electric Company, USA), and the grey values of the protein bands were analysed by ImageJ software.

Primary antibodies included the following: PSAT1 (ab96136, Abcam, Cambridge, MA, USA); ALP (ab108337, Abcam); COL1A1 (#84336, CST, Danvers, MA, USA); RUNX2 (ab23981, Abcam); Akt (pan) (#4691, CST); p-Akt (Ser473) (p-Akt) (#4060, CST); p-GSK3 β (#9323, CST); GSK-3 β (#12456, CST); β -Catenin (#8480, CST); Nonphospho (Active) β -Catenin (#8814, CST); ATF4 (#11815, CST); β -Actin (sc-517582, CST); Histone-H3 (17168-1-AP, Proteintech, Chicago, IL, USA); and GAPDH (HRP-60,004, Proteintech).

RNA isolation and quantitative real-time polymerase chain reaction (qRT-PCR)

Total RNA was extracted from cells using Total RNA Extraction Reagent (Vazyme, Nanjing, China) according to the manufacturer's instructions. Then, the RNA was reverse transcribed to cDNA using HiScript III RT SuperMix for qPCR (+gDNA wiper) (Vazyme). qRT-PCR was performed in a 10 μ L reaction volume with ChamQ Universal SYBR qPCR Master Mix (Vazyme), and the changes in gene expression were calculated by the $2^{-\Delta\Delta CT}$ method. GAPDH was used as the internal control. The primers of the genes are shown in Additional file 2.

Construction of the rat mandibular defect model

Seven-week-old male Wistar rats (200–250 g) supplied by SPF Biotechnology Co., Ltd. (Beijing, China) were kept in the animal centre of Shandong Engineering Laboratory for Dental Materials and Oral Tissue Regeneration. After 1 week of acclimation, the rats were anaesthetized by the intraperitoneal injection of pentobarbital sodium anaesthesia (40 mg/kg body weight). An incision parallel to the inferior border of the mandible was made, the skins and muscles were separated, and a defect (5 \times 3 \times 1 mm³) was made on the buccal surface of the mandible using a dental round bur at a low speed with continuous physiological saline solution irrigation. The anterior margin of the defect was 2 mm from the anterior edge of the mandible, and the lower margin was located 1 mm above the lower edge of the mandible. Then, PDLSC-bone powder mixtures from different groups were implanted into the defect and covered with biomembranes (Zhenghai Biotechnology, China) to prevent the growth of soft tissue.

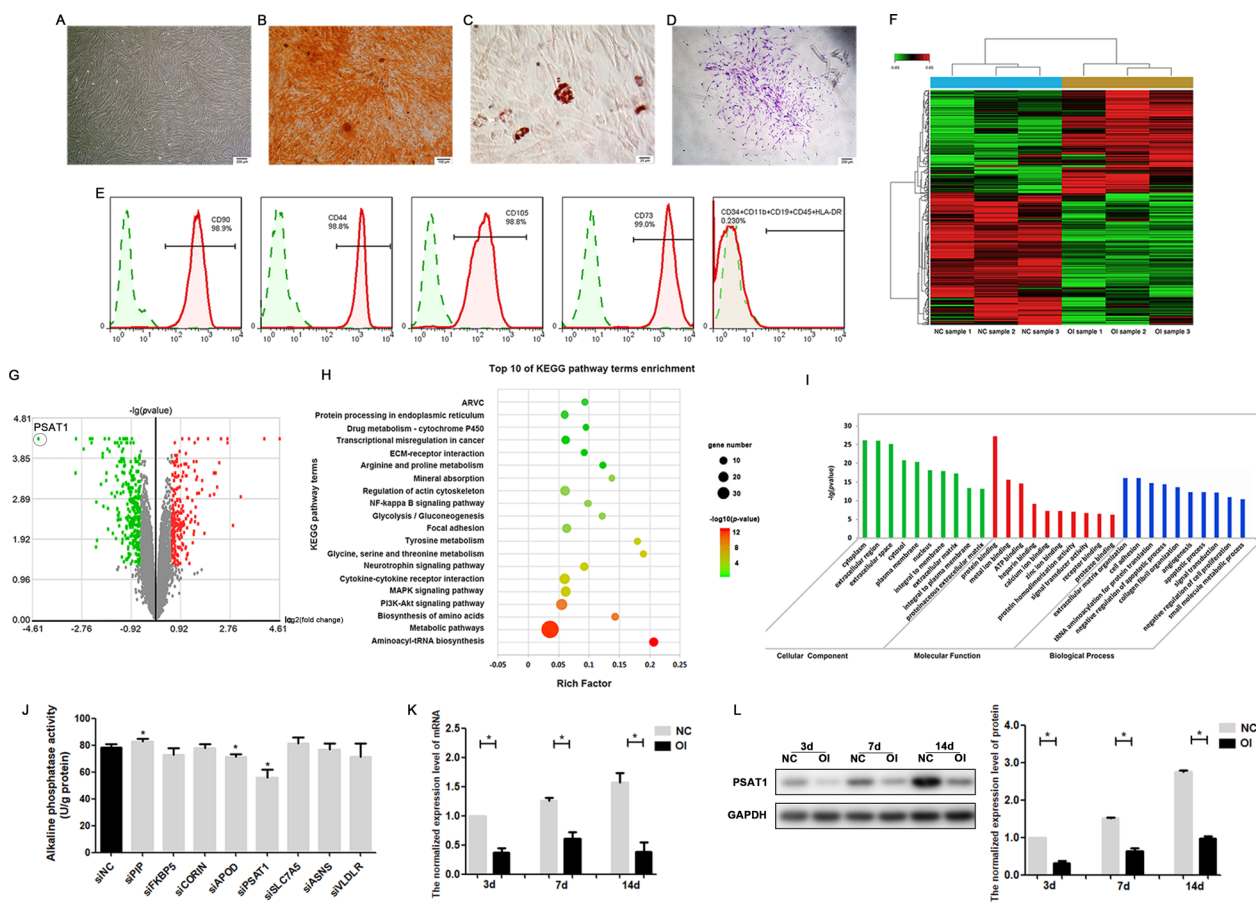


Fig. 1 Microarray and bioinformatics analyses for differentially expressed genes in PDLSCs after osteogenic induction. **A** PDLSCs cultured in vitro presented spindle-like morphology and formed spiral arrangements. **B** Alizarin Red staining of PDLSCs after osteogenic induction for 4 weeks. **C** Oil Red O staining of PDLSCs after adipogenic induction for 4 weeks. **D** Clonogenic assay of PDLSCs. **E** Immunophenotype assay of PDLSCs. **F** Clustering heatmap of differentially expressed mRNAs in PDLSCs after osteogenic induction for 7 days. **G** Volcano plot of differentially expressed mRNAs in PDLSCs after osteogenic induction for 7 days. **H** The top 10 KEGG pathways enriched by differentially expressed mRNAs in PDLSCs. **I** The top 10 GO terms enriched by differentially expressed mRNAs in PDLSCs. **J** The quantitative analysis of ALP activity in PDLSCs after siRNAs were transfected. **K** The mRNA level of *PSAT1* in PDLSCs after osteogenic induction for 3, 7, and 14 days. **L** The protein level of *PSAT1* in PDLSCs after osteogenic induction for 3, 7, and 14 days. NC: PDLSCs that were cultured in the complete culture medium. OI: PDLSCs that were cultured in the osteogenic medium. * $p < 0.05$

Finally, muscles and subcutaneous tissues were sutured layer by layer with resorbable sutures. Penicillin sodium (160,000 IU/mL) was injected intramuscularly during the first 3 days after the surgery, and a soft diet was provided for 1 week. Each group had 4 rats, and the rats were sacrificed by cardiac perfusion at 8 weeks after the surgery. Then, the mandibular specimens were harvested. The mandibular specimens were fixed in 4% paraformaldehyde for 48 h, and then prepared for microscopic computerized tomography (micro-CT) analysis, histomorphometric analysis and Masson's trichrome staining analysis.

For the preparation of the PDLSC-bone powder mixture, 4×10^6 OEPSAT1 PDLSCs, OENC PDLSCs, shP-SAT1 PDLSCs or shNC PDLSCs were cultured in

osteogenic medium for 7 days. Then, the cells were mixed with 6 mg of bone powder (BioOss, Geistlich Biomaterials, Switzerland) and incubated in a 5% CO₂ incubator at 37 °C for 6 h before surgery.

Micro-CT analysis

The mandibular specimens were scanned using a micro-CT scanner (μ CT-100, SCANCO Medical AG, Switzerland) with an effective pixel size of 15 μ m. Then, the three-dimensional images were reconstructed, and the volumetric parameters of the newly formed bone in the surgical area were analysed, including the bone volume per tissue volume (BV/TV, %), the trabecular bone thickness (Tb.-Th, mm), the trabecular bone separation (Tb.-Sp, mm), and the total number of trabeculae (Tb.N; mm).

Haematoxylin–eosin (HE) staining and Masson’s trichrome staining

The mandibular specimens were decalcified in 10% disodium ethylenediamine tetraacetate in phosphate buffer for approximately 2 months, dehydrated through a graded series of ethanol solutions and embedded in paraffin. The specimens were cut to generate series sections (5- μ m thickness) from the mesial to distal direction, which involved the whole surgical area. Respective sections of the defects were used for HE staining and Masson’s trichrome staining with the Hematoxylin–Eosin/HE Staining Kit (Solarbio) and the Masson’s Trichrome Stain Kit (Solarbio).

Chromatin immunoprecipitation (ChIP) assay

ChIP experiments were performed using the ChIP Assay Kit (Beyotime) according to the manufacturer’s instructions. An antibody against ATF4 (#11815, CST) was applied, and rabbit IgG (A7016, Beyotime) was used as a control. The ChIP products were amplified by qRT-PCR. The primers for qRT-PCR were as follows: forward primer (5’–3’) GGCGCATCAATTTTACTCAGAC; reverse primer (5’–3’) CAGAATACCCTCCCCCTACCC.

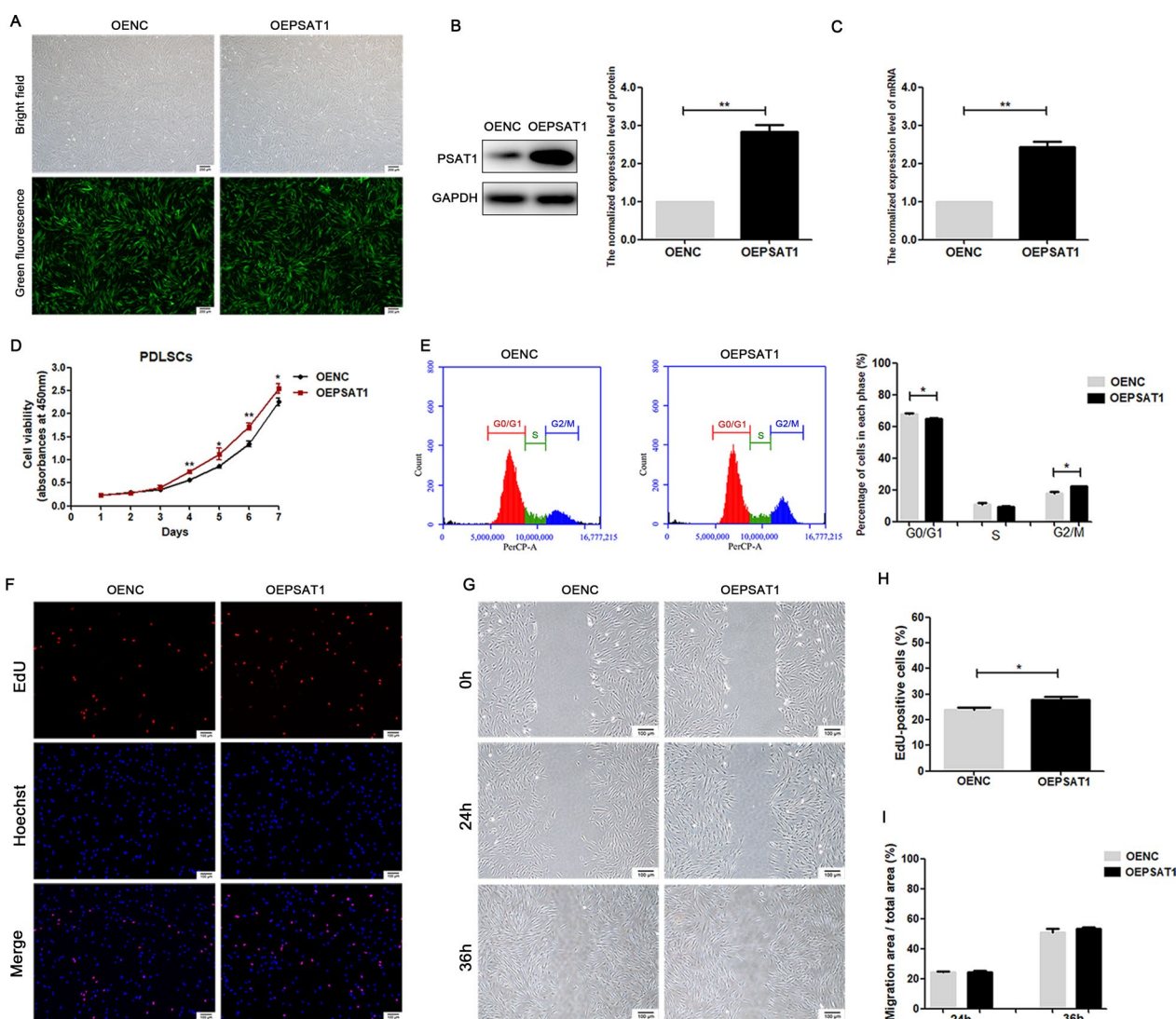


Fig. 2 The effect of *PSAT1* overexpression on proliferation activity and migration ability of PDLSCs. **A** PDLSCs transfected with lentivirus were observed under fluorescence microscope. **B, C** The expression levels of *PSAT1* protein and *PSAT1* mRNA in PDLSCs were detected by Western Blot and qRT-PCR. **D** Cell viability of PDLSCs was detected by CCK-8. **E** The distribution of the cell cycle in PDLSCs was detected by flow cytometry. **F, H** Cell proliferation activity of PDLSCs was detected by EdU, and the proportion of EdU-positive cells was calculated. **G, I** Migration ability of PDLSCs was analyzed, and the migration efficiency was calculated. OEPSAT1: PDLSCs with *PSAT1* overexpressed. OENC: control PDLSCs. * $p < 0.05$; ** $p < 0.01$

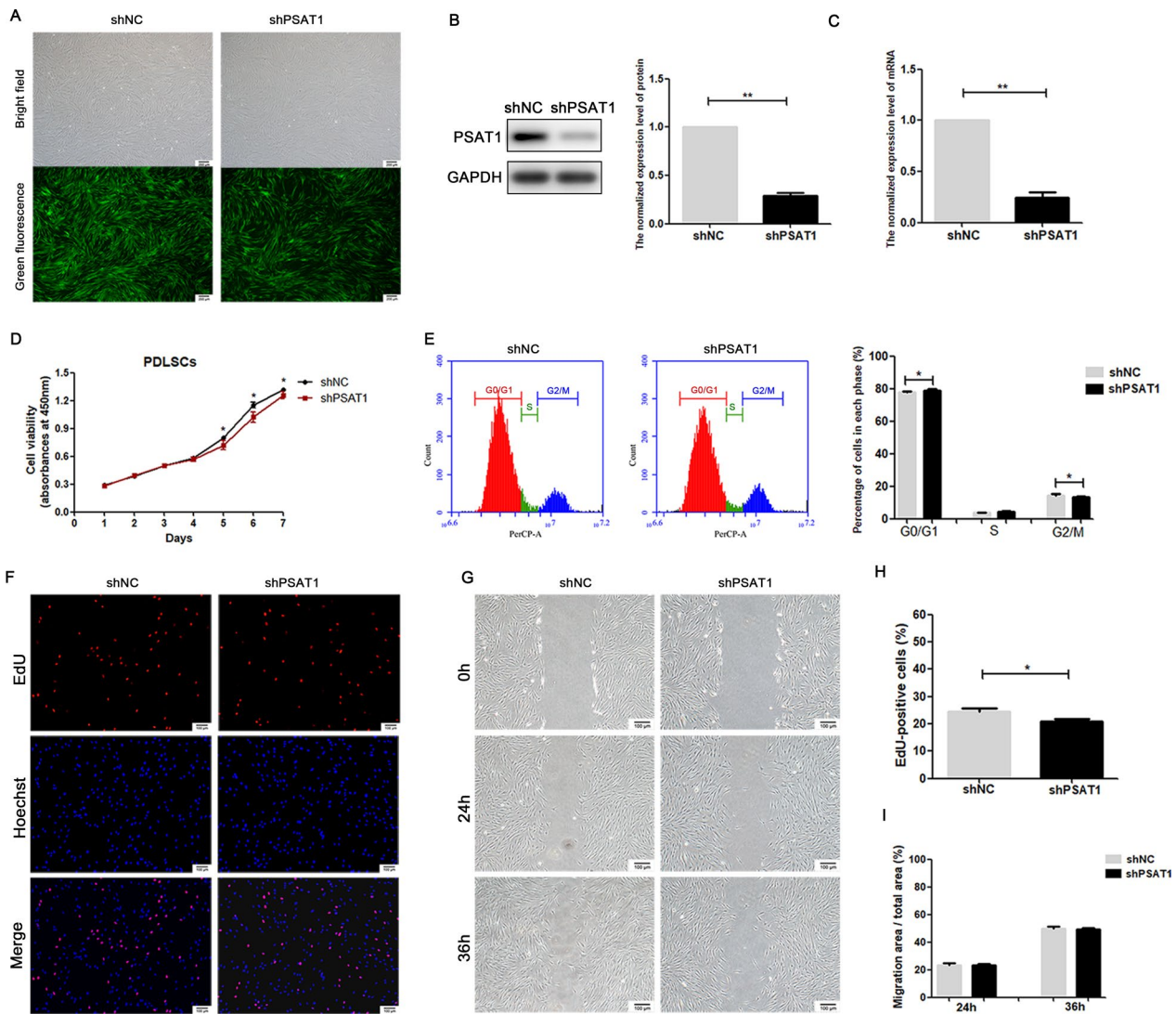


Fig. 3 The effect of *PSAT1* knockdown on proliferation activity and migration ability of PDLSCs. **A** PDLSCs transfected with lentivirus were observed under fluorescence microscope. **B, C** The expression levels of *PSAT1* protein and *PSAT1* mRNA in PDLSCs were detected by Western Blot and qRT-PCR. **D** Cell viability of PDLSCs was detected by CCK-8. **E** The distribution of the cell cycle in PDLSCs was detected by flow cytometry. **F, H** Cell proliferation activity of PDLSCs was detected by EdU, and the proportion of EdU-positive cells was calculated. **G, I** Migration ability of PDLSCs was analyzed, and the migration efficiency was calculated. shPSAT1: PDLSCs with *PSAT1* knocked down. shNC: control PDLSCs. * $p < 0.05$; ** $p < 0.01$

Statistical analysis

All experiments were repeated at least three times, and all data are presented as the means \pm standard deviations. Student's t test or one-way ANOVA was used to determine significant differences between experimental and control values. The statistical analyses were conducted using GraphPad software, and values of $p < 0.05$ were considered significant.

Results

Culture and identification of PDLSCs

PDLSCs cultured in vitro exhibited spindle-like morphology and formed spiral arrangements (Fig. 1A). In the multilineage differentiation assay, PDLSCs produced Alizarin Red-positive mineralized matrix (Fig. 1B) or Oil Red O-positive lipid droplets (Fig. 1C) after being cultured in osteogenic or adipogenic medium for 4 weeks,

which confirmed that PDLSCs possessed the ability of osteogenic and adipogenic differentiation. In the clonogenic assay, PDLSCs showed strong proliferative ability, and each cell could form a colony composed of more than 50 cells (Fig. 1D). In the immunophenotype assay, PDLSCs positively expressed mesenchymal cell specific surface markers such as CD73, CD90, CD105 and CD44, and negatively expressed haematopoietic or endothelial-specific antigens including CD34, CD11b, CD19, CD45 and HLA-DR (Fig. 1E). All above results proved that the PDLSCs obtained in this experiment were consistent with the characteristics of MSCs.

Microarray and bioinformatics analyses for differentially expressed genes in PDLSCs after osteogenic induction

To identify potential regulators of osteogenic differentiation in PDLSCs, we used a GeneChip microarray assay to compare the mRNA expression profiles between osteodifferentiated PDLSCs and control PDLSCs. According to the requirements of $p < 0.05$ and the absolute value of FC ≥ 1.5 , the expression levels of 499 genes in PDLSCs were screened to change significantly after osteogenic induction, including 219 upregulated and 280 downregulated (Fig. 1F, G, Additional file 3). To verify the accuracy of the microarray assay, qRT-PCR was used to further detect the expression level of these screened genes. The results of qRT-PCR on 6 representative genes were highly consistent with those of microarray data, suggesting that the microarray assay was reliable (Additional file 4).

GO analyses and pathway analyses were performed to understand the function of differentially expressed genes in PDLSCs. In GO analyses, all of the differentially expressed genes participated in 326 BP terms, 50 CC terms and 88 MF terms. According to the p value, the top 10 GO terms are shown in Fig. 1I. In pathway analyses, all of the differentially expressed genes were enriched in 89 significant signalling pathways, and the top 10 terms according to p value are shown in Fig. 1H, which showed that pathways such as metabolic pathways, the PI3K-Akt signalling pathway, the MAPK signalling pathway, and cytokine–cytokine receptor interaction pathway could play regulatory roles in the osteogenic lineage differentiation of PDLSCs.

Based on all of the above results, the screened differentially expressed genes with high FC were thought to be more likely to be related to the osteogenic differentiation of PDLSCs. To further screen genes that play important roles, siRNAs were used to inhibit the expression of 8 representative genes with high FC (*PIP*, *FKBP5*, *CORIN*, *APOD*, *PSAT1*, *SLC7A5*, *ASNS*, and *VLDLR*) in PDLSCs during osteogenic induction (Additional file 5). As shown in Fig. 1J, the ALP activity of PDLSCs decreased significantly after *PSAT1* was knocked down, suggesting that *PSAT1* may participate in the regulation of osteogenic differentiation. We detected *PSAT1* mRNA and PSAT1 protein on the 3rd, 7th and 14th day of osteogenic induction, and found that *PSAT1* expression in osteodifferentiated PDLSCs was always lower than that in undifferentiated PDLSCs. Based on all of the above experiments, we speculated that *PSAT1* participated in the regulation of osteogenic differentiation in PDLSCs, and thus carried out more experiments to verify this hypothesis.

Overexpression and knockdown efficiency of *PSAT1* in PDLSCs

Lentiviral vectors with green fluorescent labels were used to overexpress or knock down *PSAT1* expression in PDLSCs. As observed under a fluorescence microscope, more than 90% of PDLSCs were successfully transfected with lentivirus (Figs. 2A, 3A). Next, the mRNA and protein expression levels of *PSAT1* in PDLSCs were measured by qRT-PCR and Western Blot. The results showed that the mRNA and protein levels of *PSAT1* were higher in OE*PSAT1* PDLSCs than in OENC PDLSCs (Fig. 2B, C), while those in sh*PSAT1* PDLSCs were lower than those in shNC PDLSCs (Fig. 3B, C), indicating that *PSAT1* was successfully overexpressed or knocked down in PDLSCs. These cells were used in the following study.

PSAT1 regulated PDLSC proliferation in vitro

Cell proliferation activity has a great influence on PDLSC-based bone regeneration; thus, CCK-8, EdU, and cell cycle flow cytometric analyses were performed to analyse the effects of overexpressing and knocking down *PSAT1* on PDLSC proliferation.

(See figure on next page.)

Fig. 4 The effect of *PSAT1* overexpression on osteogenic differentiation of PDLSCs in vitro and bone regeneration in vivo. **A** ALP staining of PDLSCs after osteogenic induction for 7 and 14 days. **B** Alizarin red staining of PDLSCs after osteogenic induction for 21 days. **C** Quantitative analysis of mineralized matrix after osteogenic induction for 21 days. **D** The quantitative analysis of ALP activity in PDLSCs after osteogenic induction. **E** The mRNA levels of *COL1A1*, *ALP* and *RUNX2* in PDLSCs after osteogenic induction. **F** The protein levels of *COL1A1*, *ALP* and *RUNX2* in PDLSCs after osteogenic induction. **G, H** Micro-CT assay of rat mandibular defect areas was performed after PDLSCs were transplanted, and the bone volume per tissue volume (BV/TV, %), the trabecular bone thickness (Tb.Th, mm), the trabecular bone separation (Tb.Sp, mm), and the total number of trabeculae (Tb.N; mm) were calculated. **I** HE staining and Masson's trichrome staining of rat mandibular defect areas. White dotted line: bone defect boundary, n: new bone, f: collagen fiber, m: jaw bone. OE*PSAT1*: PDLSCs with *PSAT1* overexpressed. OENC: control PDLSCs. * $p < 0.05$; ** $p < 0.01$

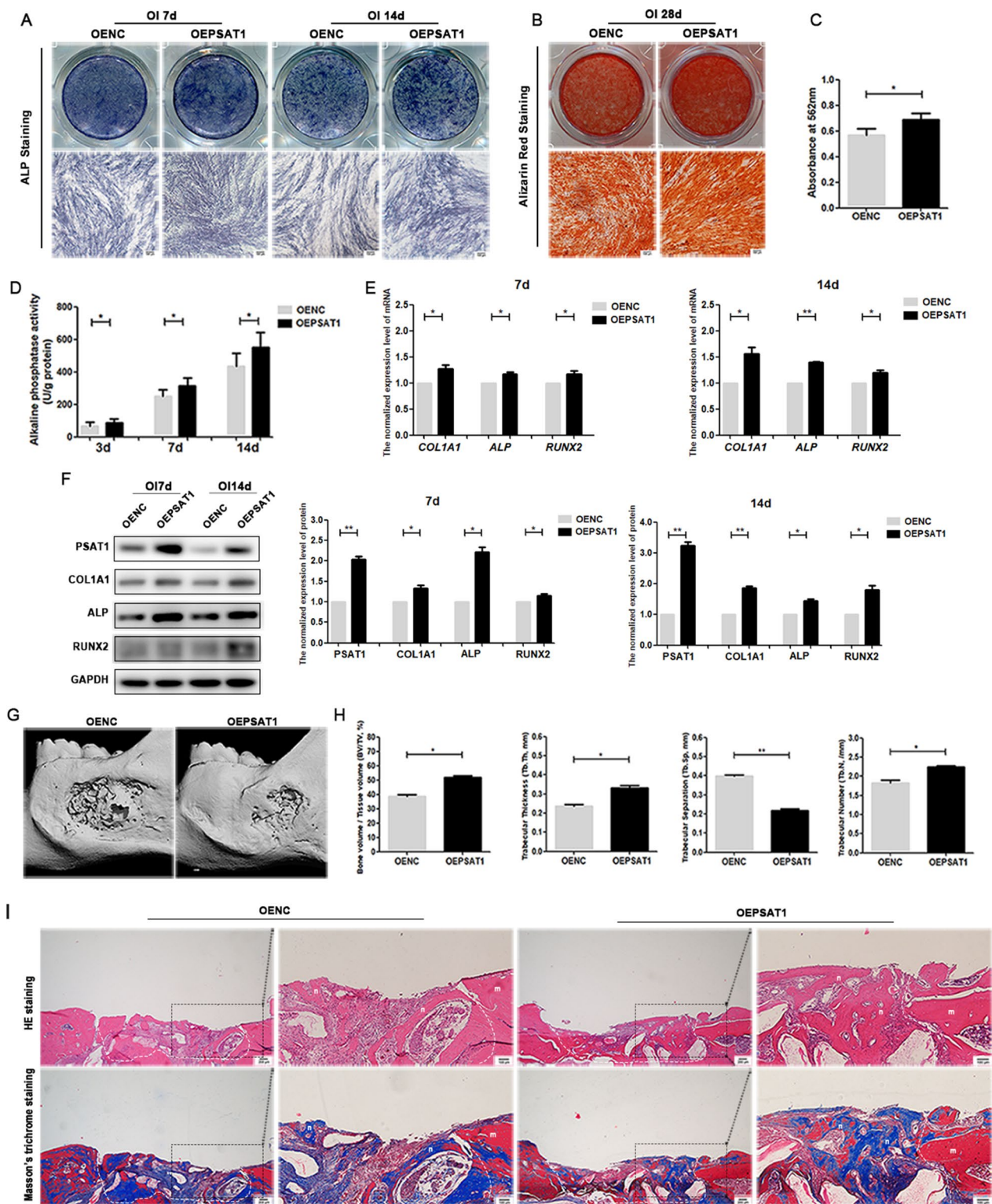


Fig. 4 (See legend on previous page.)

When *PSAT1* was overexpressed, the CCK-8 assay on 7-day growth curves showed that the cell viability of the OEPSAT1 group was significantly higher than that of the OENC group after 4 days (Fig. 2D). In the cell cycle distribution assay, the percentage of cells in G2/M phase in the OEPSAT1 group was higher than that in the OENC group (Fig. 2E). In the EdU assay, PDLSCs were cultured for 4 days before EdU labelling, and the percentage of EdU-positive cells, which are in the active stage of DNA replication, was higher in the OEPSAT1 group than in the OENC group (Fig. 2F, H). All of the above results indicated that overexpressing *PSAT1* promoted PDLSC.

When *PSAT1* was knocked down, shPSAT1 PDLSCs had lower cell viability than shNC PDLSCs after culturing for 5 days (Fig. 3D), the percentage of cells in G2/M phase in the shPSAT1 group was lower than that in the shNC group (Fig. 3E), and the EdU-positive rates of shPSAT1 PDLSCs were lower than those of shNC PDLSCs (Fig. 3F, H). These results suggested that knocking down *PSAT1* impaired the proliferative activity of PDLSCs.

***PSAT1* did not affect the migration ability of PDLSCs in vitro**

The migration ability of seed cells is of great significance to tissue regeneration. To detect whether *PSAT1* affected the migration ability of PDLSCs, the migration area of PDLSCs was measured at 24 and 36 h after scratching. The results showed no significant difference in cell migration areas between the OENC group and the OEPSAT1 group at the above two time points (Fig. 2G, I). When *PSAT1* was knocked down, the migration areas of cells in the shPSAT1 group and the shNC group were similar (Fig. 3G, I). Thus, overexpression or knockdown of *PSAT1* had no significant effect on PDLSC migration.

***PSAT1* regulated the osteogenic differentiation of PDLSCs in vitro**

To study the regulation effects of *PSAT1* on the osteogenic differentiation ability of PDLSCs, OENC, OEPSAT1, shNC and shPSAT1 PDLSCs were cultured in osteogenic medium for 21 days.

When comparing OENC PDLSCs and OEPSAT1 PDLSCs, the ALP activity of OEPSAT1 PDLSCs on Days

3, 7, and 14 was stronger than that of OENC PDLSCs (Fig. 4D). Correspondingly, the ALP staining of the OEPSAT1 group on Days 7 and 14 was also deeper than that of the OENC group (Fig. 4A). The results of Alizarin red staining and quantitative analysis showed that OEPSAT1 PDLSCs formed more mineralized matrix than OENC PDLSCs after osteogenic induction for 21 days (Fig. 4B, C). The expression of osteogenic differentiation markers such as *ALP*, *COL1A1* and *RUNX2* was also detected, and the results showed that the protein and mRNA levels of these markers in OEPSAT1 PDLSCs were higher than those in OENC PDLSCs (Fig. 4E, F). Thus, *PSAT1* overexpression enhanced the osteogenic differentiation ability of PDLSCs.

When *PSAT1* was knocked down, the ALP activity of shPSAT1 PDLSCs was weaker than that of shNC PDLSCs (Fig. 5D). The ALP staining of shPSAT1 PDLSCs was also lighter than that of shNC PDLSCs (Fig. 5A). Less mineralized matrix was formed in the shPSAT1 group than in the shNC group (Fig. 5B, C). In addition, the protein and mRNA expression of *ALP*, *COL1A1*, and *RUNX2* in shPSAT1 PDLSCs was lower than that in shNC PDLSCs (Fig. 5E, F). These results indicated that knocking down *PSAT1* inhibited the osteogenic differentiation of PDLSCs.

***PSAT1* influenced PDLSC-mediated bone regeneration in vivo**

To investigate the influence of *PSAT1* on PDLSC-mediated bone regeneration, PDLSCs with *PSAT1* overexpression or knockdown were transplanted into rat mandibular defect areas, and then micro-CT, HE staining and Masson's trichrome staining were used to analyze the healing of the defects and evaluate the quantity and quality of newly formed bone.

When *PSAT1* was overexpressed, the micro-CT results at 8 weeks showed that the OEPSAT1 group had a higher BV/TV value, a higher Tb.-Th value, a higher Tb.-N value, and a lower Tb.-Sp value than the OENC group (Fig. 4G, H). In the HE staining assay, more newly formed bones were observed in the OEPSAT1 group than in the OENC group (Fig. 4I). In the Masson's trichrome staining assay, more newly formed bones,

(See figure on next page.)

Fig. 5 The effect of *PSAT1* knockdown on osteogenic differentiation of PDLSCs in vitro and bone regeneration in vivo. **A** ALP staining of PDLSCs after osteogenic induction for 7 and 14 days. **B** Alizarin red staining of PDLSCs after osteogenic induction for 21 days. **C** Quantitative analysis of mineralized matrix after osteogenic induction for 21 days. **D** The quantitative analysis of ALP activity in PDLSCs after osteogenic induction. **E** The mRNA levels of *COL1A1*, *ALP* and *RUNX2* in PDLSCs after osteogenic induction. **F** The protein levels of *COL1A1*, *ALP* and *RUNX2* in PDLSCs after osteogenic induction. **G, H** Micro-CT assay of rat mandibular defect areas was performed after PDLSCs were transplanted, and the bone volume per tissue volume (BV/TV, %), the trabecular bone thickness (Tb. Th, mm), the trabecular bone separation (Tb.Sp, mm), and the total number of trabeculae (Tb.N; mm) were calculated. **I** HE staining and Masson's trichrome staining of rat mandibular defect areas. White dotted line: bone defect boundary, n: new bone, f: collagen fiber, m: jaw bone. shPSAT1: PDLSCs with *PSAT1* knocked down. shNC: control PDLSCs. * $p < 0.05$; ** $p < 0.01$

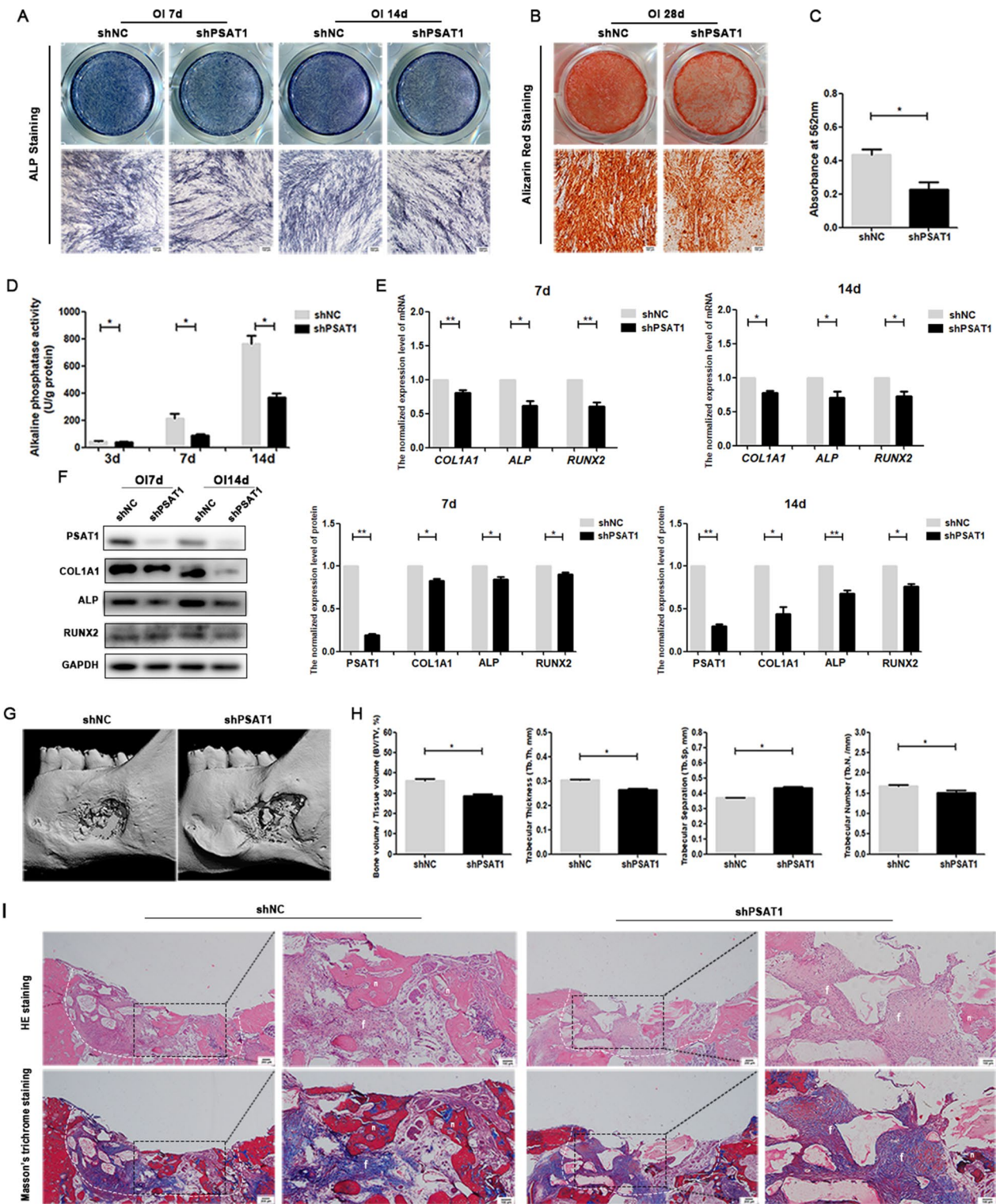


Fig. 5 (See legend on previous page.)

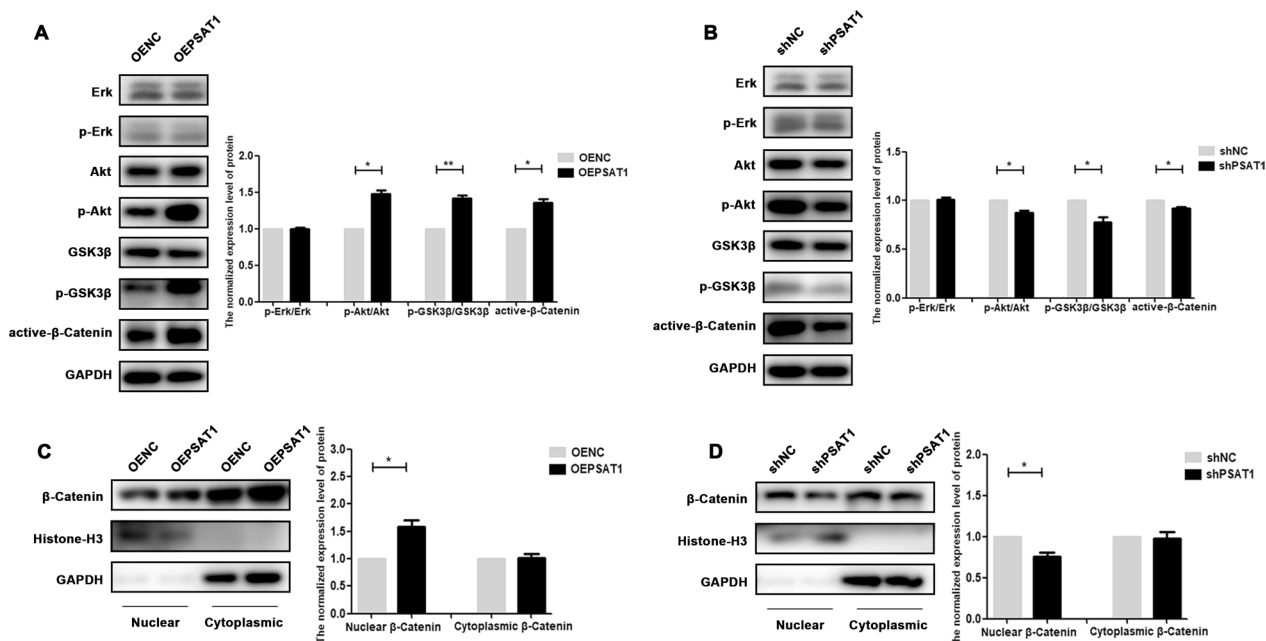


Fig. 6 *PSAT1* regulated Akt/GSK3β/β-catenin signaling pathway in PDLSCs. **A** The phosphorylation level of Erk, Akt, and GSK3β, and the protein level of active-β-catenin were analyzed in PDLSCs with *PSAT1* overexpressed. **B** The phosphorylation level of Erk, Akt, and GSK3β, and the protein level of active-β-catenin were analyzed in PDLSCs with *PSAT1* knocked down. **C** Western Blot analysis of β-Catenin protein in nucleus and cytoplasm after *PSAT1* was overexpressed. **D** Western Blot analysis of β-Catenin protein in nucleus and cytoplasm after *PSAT1* was knocked down. OEPSAT1: PDLSCs with *PSAT1* overexpressed. OENC: control PDLSCs for OEPSAT1 PDLSCs. shPSAT1: PDLSCs with *PSAT1* knocked down. shNC: control PDLSCs for shPSAT1 PDLSCs. **p* < 0.05; ***p* < 0.01

which were rich in collagen type I stained blue, were detected in the OEPSAT1 group than in the OENC group (Fig. 4I). All of the above results suggested that overexpressing *PSAT1* improved PDLSC-based bone regeneration in the mandibular defect model.

When comparing the shNC and shPSAT1 groups, a decrease in the BV/TV value, Tb.-Th value, and Tb.-N value, and an increase in Tb.-Sp values were observed in the shPSAT1 group in the micro-CT assay (Fig. 5G, H). The results of HE staining showed that newly formed bones were less abundant in the shPSAT1 group than in the shNC group (Fig. 5I). In the Masson’s trichrome staining assay, fewer new bones were formed in the shPSAT1 group than in the shNC group, which was consistent with the results of HE staining (Fig. 5I). All of these results indicated that knocking down *PSAT1* impaired PDLSC-based bone regeneration in mandibular defect area.

***PSAT1* regulated the osteogenic differentiation of PDLSCs through the Akt/GSK3β/β-catenin signalling pathway**

As mentioned above, the differentially expressed genes in PDLSCs after osteogenic induction were enriched in different signalling pathways, including the MAPK signalling pathway, and the PI3K/Akt signalling pathway. To

explore the potential regulatory mechanisms of *PSAT1*, the phosphorylation of Erk and Akt, which reflect the activity of MAPK/Erk signalling and PI3K/Akt signalling respectively, was detected. As shown in Fig. 6A, B, the phosphorylation level of Erk in PDLSCs did not change significantly when *PSAT1* was overexpressed or knocked down. When the phosphorylation level of Akt was detected, it increased or decreased with the overexpression or knockdown of *PSAT1* (Fig. 6A, B). We further detected the expression of downstream factors of Akt signalling, including GSK3β and β-catenin. The Western Blot results showed that the phosphorylation level of GSK3β and the protein level of active-β-catenin (non-phospho β-catenin) in PDLSCs increased when *PSAT1* was overexpressed (Fig. 6A), while they decreased when *PSAT1* was knocked down (Fig. 6B). Consistent with the above results, the amount of β-catenin protein in the cell nucleus increased due to the overexpression of *PSAT1* (Fig. 6C), while it decreased when *PSAT1* was knocked down (Fig. 6D). All of the above results suggested that *PSAT1* could promote the conduction of Akt/GSK3β/β-catenin signals in PDLSCs.

To further validate whether *PSAT1* regulated the osteogenic differentiation of PDLSCs through the Akt/GSK3β/β-catenin signalling pathway, LY294002 or SC79, which

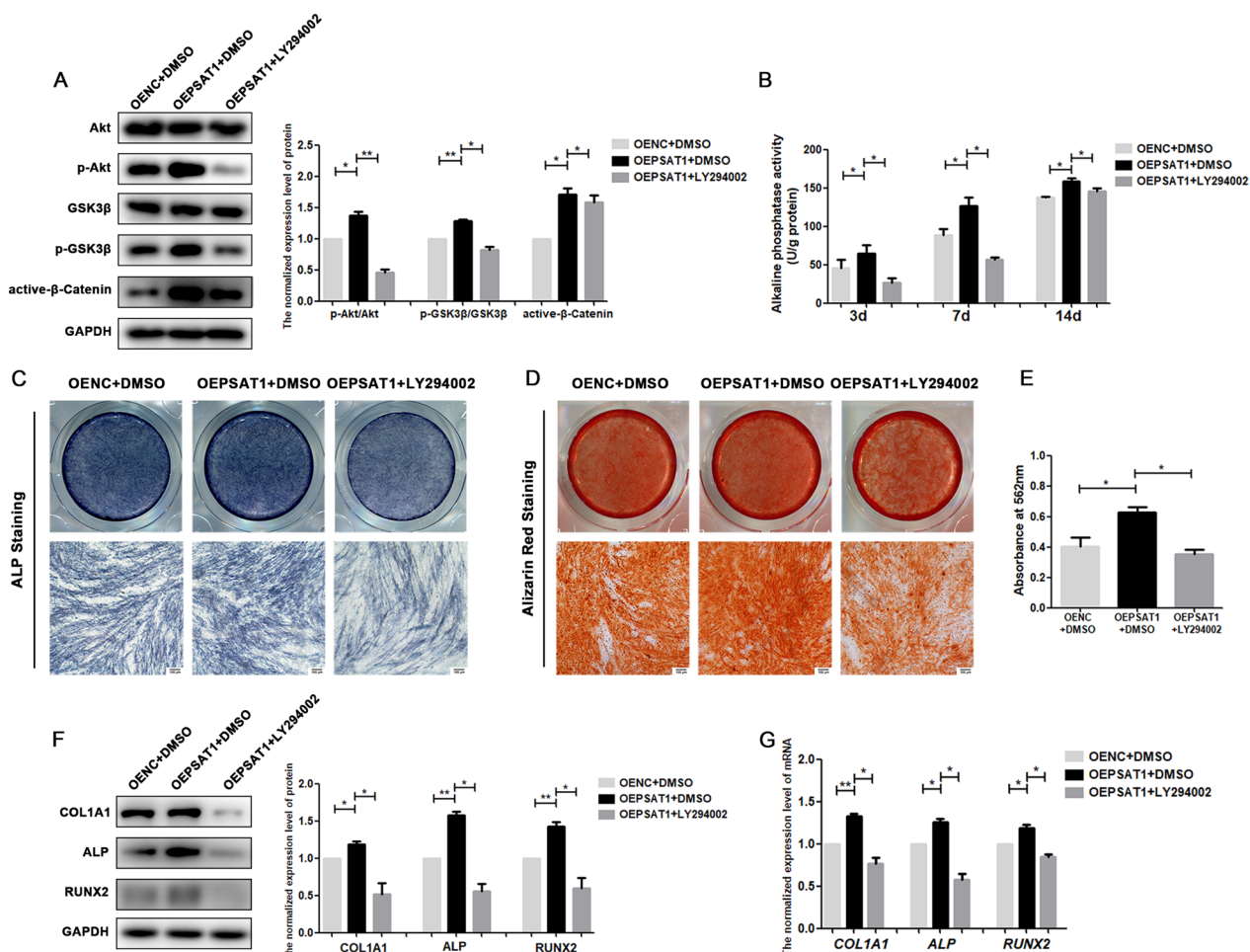


Fig. 7 LY294002 reversed the effects of overexpressing *PSAT1* on the osteogenic differentiation of PDLSCs. **A** The phosphorylation level of Akt and GSK3 β , and the protein level of active- β -catenin were analyzed in PDLSCs. **B** The quantitative analysis of ALP activity in PDLSCs after osteogenic induction. **C** ALP staining of PDLSCs after osteogenic induction for 7 days. **D** Alizarin red staining of PDLSCs after osteogenic induction for 21 days. **E** Quantitative analysis of mineralized matrix after osteogenic induction for 21 days. **F** The protein levels of COL1A1, ALP and RUNX2 in PDLSCs after osteogenic induction for 7 days. **G** The mRNA levels of *COL1A1*, *ALP* and *RUNX2* in PDLSCs after osteogenic induction for 7 days. OEPSAT1: PDLSCs with *PSAT1* overexpressed. OENC: control PDLSCs. * $p < 0.05$; ** $p < 0.01$

can inhibit or promote the phosphorylation of Akt, was applied during the osteogenic induction of PDLSCs. As shown in Fig. 7A, the phosphorylation of Akt in the OEPSAT1 group was higher than that in the OENC group, but when LY294002 was added to the medium of the OEPSAT1 group, the higher phosphorylation level of Akt in OEPSAT1 PDLSCs was reduced (Fig. 7A). In the following experiments, LY294002 led to a decrease in ALP activity (Fig. 7B), ALP staining (Fig. 7C), mineralization of extracellular matrix (Fig. 7D, E), and expression of osteogenic differentiation markers (Fig. 7F, G) in the OEPSAT1 plus LY294002 group compared to the OEPSAT1 group, which suggested that inhibiting the phosphorylation of Akt could reverse the enhancement

of osteogenic differentiation caused by overexpressing *PSAT1*. In addition, compared with the shPSAT1 group, the phosphorylation of Akt in shPSAT1 plus SC79 group increased (Fig. 8A), and stronger ALP activity (Fig. 8B, C), more mineralization of the extracellular matrix (Fig. 8D, E), and higher expression levels of osteogenic differentiation markers (Fig. 8F, G) were observed in the shPSAT1 plus SC79 group, which indicated that improving the phosphorylation level of Akt could reverse the decrease in osteogenic differentiation caused by the knockdown of *PSAT1*. All of the above results proved that overexpressing or knocking down *PSAT1* could regulate the osteogenic differentiation of PDLSCs through the Akt/GSK3 β / β -catenin signalling pathway.

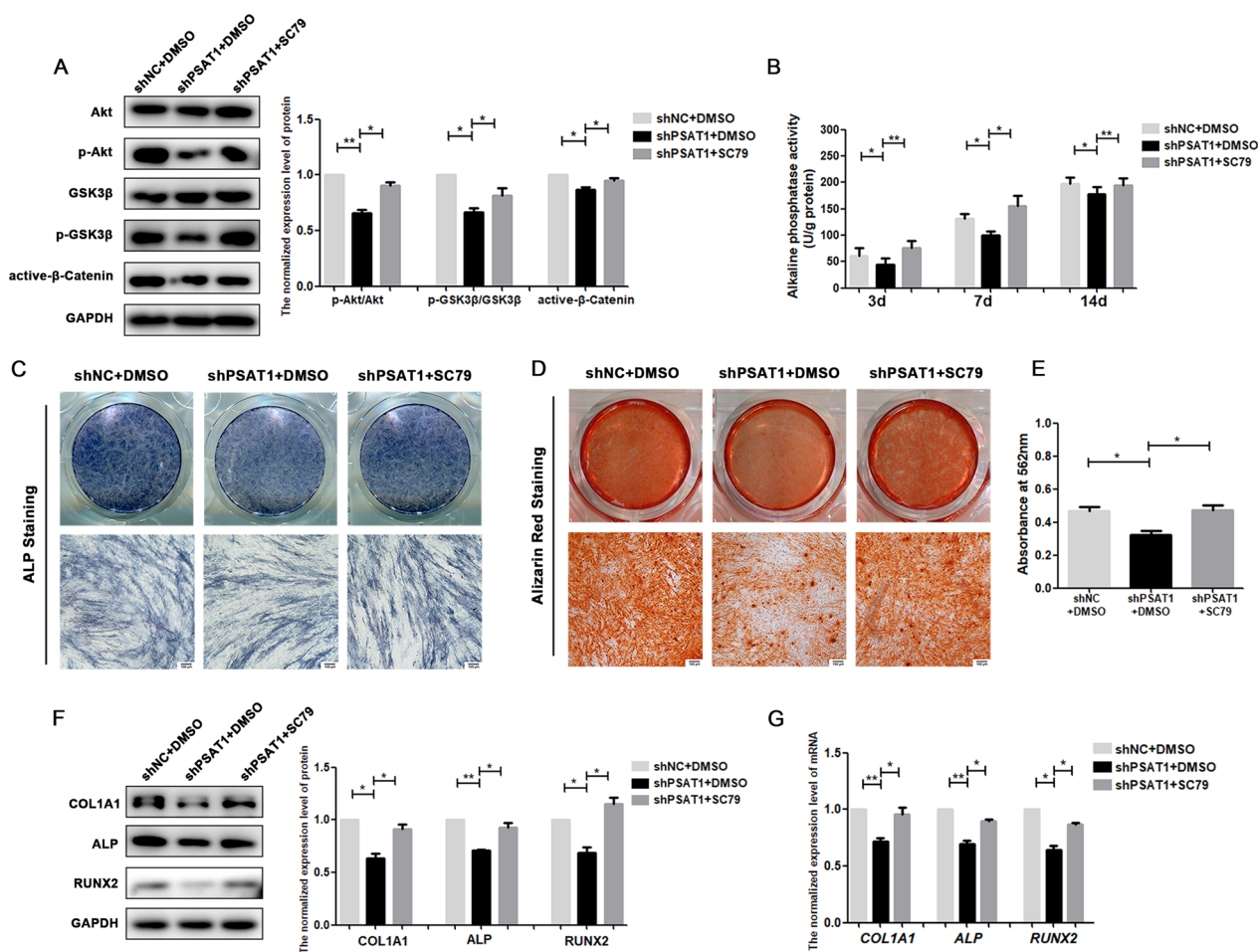


Fig. 8 SC79 reversed the effects of knocking down *PSAT1* on the osteogenic differentiation of PDLSCs. **A** The phosphorylation level of Akt and GSK3β, and the protein level of active-β-catenin were analyzed in PDLSCs. **B** The quantitative analysis of ALP activity in PDLSCs after osteogenic induction. **C** ALP staining of PDLSCs after osteogenic induction for 7 days. **D** Alizarin red staining of PDLSCs after osteogenic induction for 21 days. **E** Quantitative analysis of mineralized matrix after osteogenic induction for 21 days. **F** The protein levels of COL1A1, ALP and RUNX2 in PDLSCs after osteogenic induction for 7 days. **G** The mRNA levels of COL1A1, ALP and RUNX2 in PDLSCs after osteogenic induction for 7 days. shPSAT1: PDLSCs with *PSAT1* knocked down. shNC: control PDLSCs. **p* < 0.05; ***p* < 0.01

***PSAT1* expression was regulated by the transcription factor ATF4**

To further clarify the signal network mediated by *PSAT1* in PDLSCs, we analysed the results of the microarray assay and screened 11 genes had coexpression relationships with *PSAT1* (Additional file 6). Among these genes, *ATF4*, which encodes a well-known transcription factor that can regulate the biological behaviour of stem cells, had a high correlation coefficient with *PSAT1* according to the microarray assay. To explore the connection between *ATF4* and *PSAT1*, the expression levels of *PSAT1* and *ATF4* in undifferentiated PDLSCs and osteodifferentiated PDLSCs were detected by qRT-PCR and Western Blot. As shown in Fig. 9A–C, the protein and mRNA levels of *ATF4* and *PSAT1* in PDLSCs showed a similar change trend after osteogenic induction for 3 and

7 days. Next, we used a plasmid or siRNA to upregulate or inhibit *ATF4* expression in PDLSCs, and found that the mRNA and protein levels of *PSAT1* increased or decreased when *ATF4* was overexpressed or knocked down (Fig. 9D–G). In addition, *ATF4* overexpression reversed the decrease in *PSAT1* expression levels after osteogenic induction (Fig. 9H, I). All of these results suggested a positive correlation between the expression of *PSAT1* and *ATF4*.

Then, based on the assay of the Jasper database (<http://jaspar.genereg.net/>), PROMO database (<http://alggen.lsi.upc.es/>), and GTRD database (<http://www.gtrd.com/>), a binding site of transcription factor *ATF4* was predicted in the promoter region of *PSAT1* (Fig. 9J–L), suggesting that transcription factor *ATF4* could probably regulate the transcription of *PSAT1*. Finally, we performed ChIP

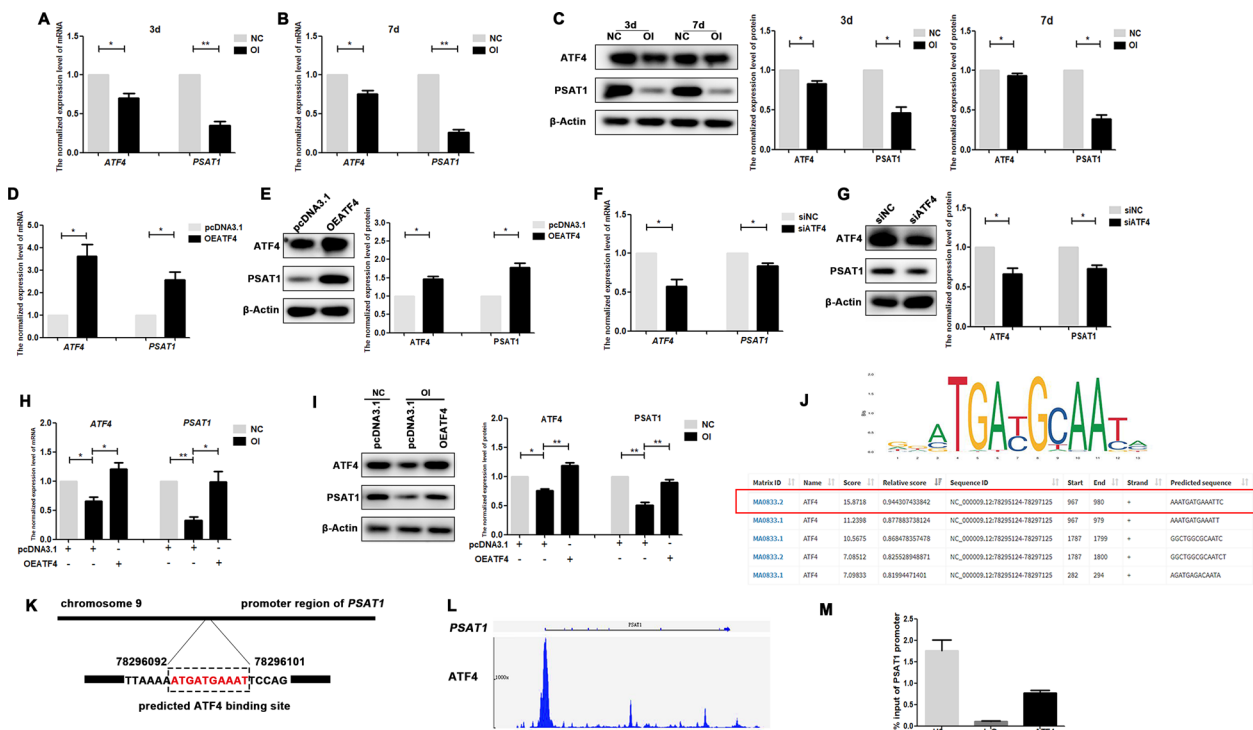


Fig. 9 The expression of *PSAT1* was regulated by transcription factor ATF4. **A, B** The mRNA levels of *ATF4* and *PSAT1* in PDLSCs after osteogenic induction for 3 and 7 days. **C** The protein levels of ATF4 and PSAT1 in PDLSCs after osteogenic induction for 3 and 7 days. **D, E** The mRNA and protein levels of *ATF4* and *PSAT1* in PDLSCs after *ATF4* was overexpressed. **F, G** The mRNA and protein levels of *ATF4* and *PSAT1* in PDLSCs after *ATF4* was interfered. **H, I** The mRNA and protein levels of *ATF4* and *PSAT1* in PDLSCs with *ATF4* overexpressed after osteogenic induction for 7 days. **J** Jasper database and PROMO database were used to predict a combination of ATF4 protein and *PSAT1* promoter. **K** The predicted binding sites in promoter region of *PSAT1* that could bind to transcription factor ATF4. **L** GTRD database was used to analyze the combination peak of ATF4 and *PSAT1* promoter regions. **M** ChIP experiment verified that ATF4 could bind to the predicted region of *PSAT1*. NC: PDLSCs that were cultured in the complete culture medium. Oi: PDLSCs that were cultured in the osteogenic medium. OEATF4: PDLSCs that were transfected with the pcDNA3.1 vector containing full-length *ATF4*. pcDNA3.1: PDLSCs that were transfected with empty pcDNA3.1 vector. siATF4: PDLSCs that were transfected with siRNA-targeted *ATF4*. siNC: PDLSCs that were transfected with siRNA-targeted none. * $p < 0.05$; ** $p < 0.01$

experiments, and the results showed that transcription factor ATF4 could bind to the predicted site in the promoter region of *PSAT1* (Fig. 9M). All of the above results proved that *PSAT1* expression was regulated by ATF4 in PDLSCs, which regulated the ATF4/PSAT1/Akt/GSK3 β / β -catenin signal regulation axis during the osteogenic differentiation of PDLSCs (Fig. 10).

Discussion

As oral tissue-derived mesenchymal stem cells, PDLSCs are important candidate seed cells for bone tissue engineering to realize the regeneration of alveolar bone. Understanding the gene regulation mechanism of osteogenic differentiation in PDLSCs is critical for PDLSC-based bone regeneration. Microarray analysis based on a high-throughput platform has become a promising and efficient tool to search for meaningful genes that regulate the characteristics and functions of stem cells, and has been widely used by many scholars [32, 33]. The present

study compared the gene expression profiles of undifferentiated and osteodifferentiated PDLSCs through a microarray assay, and then filtered 499 genes whose expression levels were altered significantly after osteogenic differentiation. It is possible that these differentially expressed genes participate in the regulation of osteogenic differentiation of PDLSCs. Indeed, *PSAT1*, one of these differentially expressed genes after osteogenic induction in PDLSCs, was proven to affect the osteogenic differentiation of PDLSCs through subsequent validation experiments. Thus, the results of the microarray assay provided clues for seeking potential regulators of osteogenic differentiation, and whether the other differentially expressed genes can regulate the osteogenesis of PDLSCs requires further study.

The present study proved that overexpressing *PSAT1* promoted the osteogenic differentiation of PDLSCs in vitro and in vivo, while knocking down *PSAT1* led to impaired osteogenesis. Therefore, we speculate that

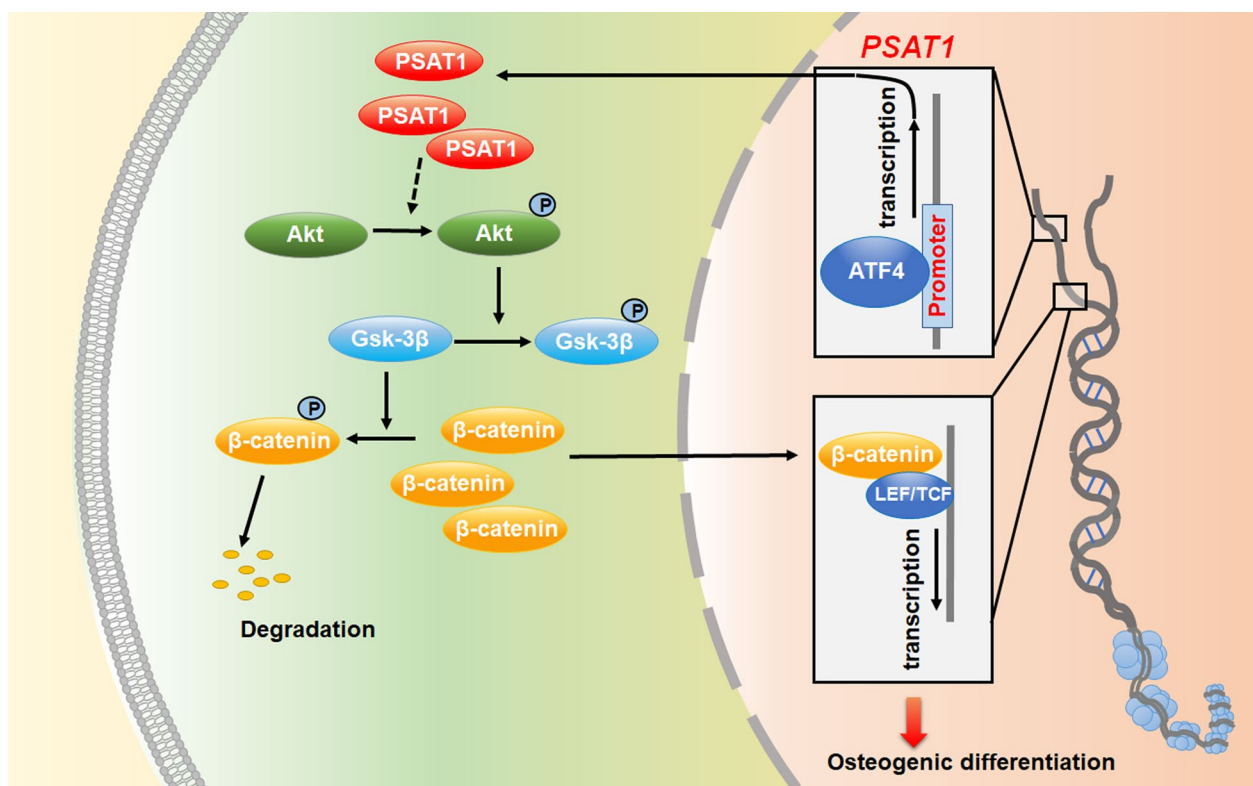


Fig. 10 Schematic diagram. *PSAT1* could regulate the osteogenic differentiation of PDLSCs through Akt/GSK3β/β-catenin signaling pathway, and the transcription of *PSAT1* is modulated by transcription factor ATF4

PSAT1 is a positive regulator of the osteogenic differentiation of PDLSCs. In fact, there have been few studies on the regulation of *PSAT1* on the osteogenic differentiation of stem cells to date. Several scholars noted that *PSAT1* expression showed a sustained and significant change during the process of mineralization in osteoblasts and periodontal ligament cells, but the possible regulatory roles of *PSAT1* were not studied [29, 34]. Here, we comprehensively verified the regulatory effect of *PSAT1* on the osteogenic differentiation of PDLSCs first, providing new ideas for enhancing PDLSC-mediated bone regeneration. Notably, a few new clues suggest that *PSAT1* may affect other behaviour of stem cells: the ability of mouse ESCs to differentiate to ectodermal lineage was impaired when *Psat1* was knocked down [28]; the serine metabolism that *PSAT1* participated in controlled dental pulp stem cell ageing [30]. Therefore, *PSAT1* could be a potential important regulator of the biological characteristics of stem cells in many aspects, which is worthy of further research in the future.

The Akt signalling pathway has been reported to regulate the biological behaviour of stem cells [35, 36]. Generally, the activated Akt signal (phosphorylated Akt)

inhibits GSK3β by phosphorylating it at Ser9, in turn promoting the stabilization and nuclear translocation of β-catenin, which could regulate the expression of downstream genes together with LEF/TCF and promote the osteogenic differentiation of stem cells [37, 38]. The present study proved that overexpressing *PSAT1* increased the phosphorylation level of Akt and promoted the activation of Akt/GSK3β/β-catenin signalling in PDLSCs, while knocking down *PSAT1* inhibited it. In addition, the inhibitor or activator of Akt signalling, LY294002 or SC79, reversed the effects of *PSAT1* overexpression or knockdown on the osteogenesis of PDLSCs, respectively. These results indicate that *PSAT1* could regulate the osteogenic differentiation of PDLSCs through the Akt/GSK3β/β-catenin signalling pathway. Our findings were similar to some previous studies on cancer; for example, *PSAT1* was reported to regulate β-catenin/cyclin D1 signalling in breast cancer cells [39], *PSAT1* was proven to affect the GSK3β/Snail pathway in esophageal cancer cells [40], and *PSAT1* could influence the PI3K/AKT pathway in cervical cancer cells [41]. Thus, *PSAT1* seems to have a wide influence on regulatory networks in different types of tissue cells. Notably, whether *PSAT1*

affects the osteogenic differentiation of PDLSCs through other mechanisms remains unclear. Given that *PSATI* is involved in the biosynthesis of serine in cells, several studies have supported that *PSATI* regulates the behaviour of cancer cells by regulating serine production [42, 43]. A study on mouse ESCs revealed that *Psat1* affected the timing of ESC differentiation by regulating the intracellular α -Ketoglutarate level instead of serine [28]. Regardless, the regulatory mechanism of *PSATI* may be diverse and needs further study.

The proliferation and self-renewal abilities of stem cells are also quite important for tissue engineering, because regeneration therapy generally requires a sufficient number of seed cells [44, 45]. Our results of CCK-8, EdU, and cell cycle assays proved that *PSATI* positively regulated PDLSC proliferation, which could contribute to PDLSC-based bone tissue engineering. In fact, several scholars have found a connection between *PSATI* and cell proliferation in some tumour cells. Nadia reported that the overexpression of *PSATI* significantly stimulated the cell growth of colon cancer cells [24]. Yang proved that *PSATI* strongly promoted the cell cycle progression and cell proliferation of non-small cell lung cancer cells [25]. Yan proved that downregulating *PSATI* expression significantly inhibited the growth of esophageal cancer cells [46]. Notably, our results showed that the effect of *PSATI* on PDLSCs proliferative activity was not as strong as previously reported in tumour cells [24, 25, 46]. This suggests that the regulation of *PSATI* on cell behaviour could vary with cell type.

The present study found that *PSATI* expression in PDLSCs decreased during osteogenic differentiation. Similarly, Hwang reported that *Psat1* was highly expressed in mouse ESCs and decreased during differentiation and suggested that maintaining *Psat1* levels could be essential for the self-renewal and pluripotency of mouse ESCs [28]. Therefore, we speculated that *PSATI* might also be related to the stemness of PDLSCs, which may explain the decreased *PSATI* expression in osteodifferentiated PDLSCs. In addition, we further proved that ATF4 could bind to the promoter region of *PSATI* and regulate its translation in PDLSCs. As a transcription factor, ATF4 has been proven to be involved in a variety of physiological and metabolic processes and can regulate the biological behaviour of stem cells [47, 48]. Several studies revealed that ATF4 could regulate the osteogenic differentiation of PDLSCs [49, 50]. Since the expression of ATF4 in PDLSCs also decreased with osteogenic differentiation, we speculated that ATF4 was one of the direct regulators that mediated the downregulation of *PSATI* expression after osteogenic induction in PDLSCs. Our findings are similar to previous studies that reported

that ATF4 could influence *PSATI* expression in some cancer cells [43, 51]. Considering that PDLSCs are quite different from these cancer cells, more exploration is required to explain the regulatory network involved in *PSATI* in PDLSCs.

Conclusion

Exploring the gene regulation mechanism for the osteogenic differentiation of PDLSCs is of great significance for PDLSC-based bone regeneration. The present study proved that *PSATI* expression was altered significantly after osteogenic induction and could positively regulate the proliferation and osteogenic differentiation of PDLSCs in vitro and promoted PDLSC-based bone regeneration in vivo. The regulatory effects of *PSATI* on osteogenesis could occur through the Akt/GSK3 β / β -catenin signalling pathway. In addition, the transcription factor ATF4 could bind to the promoter region of *PSATI* and regulate its expression. Collectively, *PSATI* could be a potential important regulator of the osteogenic differentiation of PDLSCs and a candidate regulatory target for promoting PDLSC-based bone tissue engineering.

Supplementary Information

The online version contains supplementary material available at <https://doi.org/10.1186/s12967-022-03775-z>.

Additional file 1: Table S1. The sequences of siRNAs.

Additional file 2: Table S2. The sequences of primers utilized for qRT-PCR.

Additional file 3: Table S3. The differentially expressed mRNAs in PDLSCs after osteogenic induction.

Additional file 4: Figure S1. Validation of microarray results in PDLSCs by qRT-PCR.

Additional file 5: Figure S2. The interference efficiency of using siRNA to interfere with target genes in PDLSCs.

Additional file 6: Table S3. Differentially expressed genes in PDLSCs that have co-expression relationships with *PSATI*.

Acknowledgements

None.

Author contributions

LLJ, DFL and XX designed the experiments. LLJ and DFL performed the cell and animal experiments. YNW performed the microarray and bioinformatic analysis. LLJ write the manuscript, DJZ and XX reviewed and corrected the manuscript. All authors read and approved the final manuscript.

Funding

This work was supported by grants from the Natural Science Foundation of Shandong Province (ZR2022QH099, ZR2021MH092), the Natural Science Foundation of China (82071148), and the Natural Science Foundation of Jiangsu Province (BK20210111).

Availability of data and materials

All datasets generated for this study are included in the article.

Declarations

Ethics approval and consent to participate

All the procedures in this study complied with the approved guidelines and were approved by the Ethics Committee of Hospital of Stomatology, Shandong University (human study—No. GR202028, animal study—No. GD202036). Informed consent was obtained from all human volunteers involved in the study.

Consent for publication

Not applicable.

Competing interests

The authors declare that they have no conflicts of interest.

Author details

¹Department of Prosthodontics, School and Hospital of Stomatology, Cheeloo College of Medicine, Shandong University, Jinan, China. ²Department of Implantology, School and Hospital of Stomatology, Cheeloo College of Medicine, Shandong University, No. 44-1 Wenhua Road West, Jinan 250012, Shandong, China. ³Shandong Key Laboratory of Oral Tissue Regeneration, Jinan, China. ⁴Shandong Engineering Laboratory for Dental Materials and Oral Tissue Regeneration, Jinan, China. ⁵Shandong Provincial Clinical Research Center for Oral Diseases, Jinan, China.

Received: 14 September 2022 Accepted: 15 November 2022

Published online: 02 February 2023

References

- Liu J, Ruan J, Weir MD, et al. Periodontal bone-ligament-cementum regeneration via scaffolds and stem cells. *Cells*. 2019;8(6):537.
- Kagami H, Agata H, Inoue M, et al. The use of bone marrow stromal cells (bone marrow-derived multipotent mesenchymal stromal cells) for alveolar bone tissue engineering: basic science to clinical translation. *Tissue Eng Part B Rev*. 2014;20(3):229–32.
- Yousefi AM, James PF, Akbarzadeh R, et al. Prospect of stem cells in bone tissue engineering: a review. *Stem Cells Int*. 2016;2016:618047.
- Zhang Y, Xing Y, Jia L, et al. An in vitro comparative study of multisource derived human mesenchymal stem cells for bone tissue engineering. *Stem Cells Dev*. 2018;27(23):1634–45.
- Zhu W, Liang M. Periodontal ligament stem cells: current status, concerns, and future prospects. *Stem Cells Int*. 2015;2015:972313.
- Chalisserry EP, Nam SY, Park SH, et al. Therapeutic potential of dental stem cells. *J Tissue Eng*. 2017;8:2041731417702531.
- Seo BM, Miura M, Gronthos S, et al. Investigation of multipotent postnatal stem cells from human periodontal ligament. *Lancet*. 2004;364(9429):149–55.
- Zhang Y, Ding N, Zhang T, et al. A tetra-PEG hydrogel based aspirin sustained release system exerts beneficial effects on periodontal ligament stem cells mediated bone regeneration. *Front Chem*. 2019;7:682.
- Yu BH, Zhou Q, Wang ZL. Periodontal ligament versus bone marrow mesenchymal stem cells in combination with Bio-Oss scaffolds for ectopic and in situ bone formation: a comparative study in the rat. *J Biomater Appl*. 2014;29(2):243–53.
- Liu Y, Zheng Y, Ding G, et al. Periodontal ligament stem cell-mediated treatment for periodontitis in miniature swine. *Stem Cells*. 2008;26(4):1065–73.
- Ding G, Liu Y, Wang W, et al. Allogeneic periodontal ligament stem cell therapy for periodontitis in swine. *Stem Cells*. 2010;28(10):1829–38.
- Komori T. Runx2, a multifunctional transcription factor in skeletal development. *J Cell Biochem*. 2002;87(1):1–8.
- Mao L, Liu J, Zhao J, et al. Effect of micro-nano-hybrid structured hydroxyapatite bioceramics on osteogenic and cementogenic differentiation of human periodontal ligament stem cell via wnt signaling pathway. *Int J Nanomed*. 2015;10:7031–44.
- Lv PY, Gao PF, Tian GJ, et al. Osteocyte-derived exosomes induced by mechanical strain promote human periodontal ligament stem cell proliferation and osteogenic differentiation via the miR-181b-5p/PTEN/AKT signaling pathway. *Stem Cell Res Ther*. 2020;11(1):295.
- Yan W, Cao Y, Yang H, et al. CB1 enhanced the osteo/dentinogenic differentiation ability of periodontal ligament stem cells via p38 MAPK and JNK in an inflammatory environment. *Cell Prolif*. 2019;52(6):e12691.
- Baek JY, Jun DY, Taub D, et al. Characterization of human phosphoserine aminotransferase involved in the phosphorylated pathway of L-serine biosynthesis. *Biochem J*. 2003;373(Pt 1):191–200.
- Yu J, Xiao F, Guo Y, et al. Hepatic phosphoserine aminotransferase 1 regulates insulin sensitivity in mice via Tribbles Homolog 3. *Diabetes*. 2015;64(5):1591–602.
- Hamanaka RB, O'Leary EM, Witt LJ, et al. Glutamine metabolism is required for collagen protein synthesis in lung fibroblasts. *Am J Respir Cell Mol Biol*. 2019;61(5):597–606.
- Brassier A, Valayannopoulos V, Bahi-Buisson N, et al. Two new cases of serine deficiency disorders treated with L-serine. *Eur J Paediatr Neurol*. 2016;20(1):53–60.
- Bourque DK, Cloutier M, Kernohan KD, et al. Neu-Laxova syndrome presenting prenatally with increased nuchal translucency and cystic hygroma: the utility of exome sequencing in deciphering the diagnosis. *Am J Med Genet A*. 2019;179(5):813–6.
- Ozeki Y, Pickard BS, Kano S, et al. A novel balanced chromosomal translocation found in subjects with schizophrenia and schizotypal personality disorder: altered L-serine level associated with disruption of PSAT1 gene expression. *Neurosci Res*. 2011;69(2):154–60.
- Ni C, Cheng RH, Zhang J, et al. Novel and recurrent PHGDH and PSAT1 mutations in chinese patients with Neu-Laxova syndrome. *Eur J Dermatol*. 2019;29(6):641–6.
- Liu B, Jia Y, Cao Y, et al. Overexpression of phosphoserine aminotransferase 1 (PSAT1) predicts poor prognosis and associates with tumor progression in human esophageal squamous cell carcinoma. *Cell Physiol Biochem*. 2016;39(1):395–406.
- Vie N, Copois V, Bascoul-Mollevis C, et al. Overexpression of phosphoserine aminotransferase PSAT1 stimulates cell growth and increases chemoresistance of colon cancer cells. *Mol Cancer*. 2008;7:14.
- Yang Y, Wu J, Cai J, et al. PSAT1 regulates cyclin D1 degradation and sustains proliferation of non-small cell lung cancer cells. *Int J Cancer*. 2015;136(4):E39–50.
- Gao S, Ge A, Xu S, et al. PSAT1 is regulated by ATF4 and enhances cell proliferation via the GSK3 β / β -catenin/cyclin D1 signaling pathway in ER-negative breast cancer. *J Exp Clin Cancer Res*. 2017;36(1):179.
- Metcalf S, Dougherty S, Krueger T, et al. Selective loss of phosphoserine aminotransferase 1 (PSAT1) suppresses migration, invasion, and experimental metastasis in triple negative breast cancer. *Clin Exp Metastasis*. 2020;37(1):187–97.
- Hwang I-Y, Kwak S, Lee S, et al. Psat1-dependent fluctuations in α -ketoglutarate affect the timing of ESC differentiation. *Cell Metabol*. 2016;24(3):494–501.
- Staines KA, Zhu D, Farquharson C, et al. Identification of novel regulators of osteoblast matrix mineralization by time series transcriptional profiling. *J Bone Miner Metab*. 2014;32(3):240–51.
- Yang RL, Huang HM, Han CS, et al. Serine metabolism controls dental pulp stem cell aging by regulating the DNA methylation of p16. *J Dent Res*. 2021;100(1):90–7.
- Tusher VG, Tibshirani R, Chu G. Significance analysis of microarrays applied to the ionizing radiation response. *Proc Natl Acad Sci USA*. 2001;98(9):5116–21.
- Qu Q, Fang F, Wu B, et al. Potential role of long non-coding RNA in osteogenic differentiation of human periodontal ligament stem cells. *J Periodontol*. 2016;87(7):e127–37.
- Gu X, Li M, Jin Y, et al. Identification and integrated analysis of differentially expressed lncRNAs and circRNAs reveal the potential ceRNA networks during PDLSC osteogenic differentiation. *BMC Genet*. 2017;18(1):100.
- Choi HD, Noh WC, Park JW, et al. Analysis of gene expression during mineralization of cultured human periodontal ligament cells. *J Periodontol Implant Sci*. 2011;41(1):30–43.

35. Ye C, Zhang W, Hang K, et al. Extracellular IL-37 promotes osteogenic differentiation of human bone marrow mesenchymal stem cells via activation of the PI3K/AKT signaling pathway. *Cell Death Dis.* 2019;10(10):753.
36. Zhang J, Liu X, Li H, et al. Exosomes/tricalcium phosphate combination scaffolds can enhance bone regeneration by activating the PI3K/Akt signaling pathway. *Stem Cell Res Ther.* 2016;7(1):136.
37. Shen YS, Chen XJ, Wuri SN, et al. Polydatin improves osteogenic differentiation of human bone mesenchymal stem cells by stimulating TAZ expression via BMP2-Wnt/beta-catenin signaling pathway. *Stem Cell Res Ther.* 2020;11(1):204.
38. Chen X, Hu C, Wang G, et al. Nuclear factor-kappaB modulates osteogenesis of periodontal ligament stem cells through competition with beta-catenin signaling in inflammatory microenvironments. *Cell Death Dis.* 2013;4:e510.
39. Gao S, Ge A, Xu S, et al. PSAT1 is regulated by ATF4 and enhances cell proliferation via the GSK3beta/beta-catenin/cyclin D1 signaling pathway in ER-negative breast cancer. *J Exp Clin Cancer Res.* 2017;36(1):179.
40. Li MK, Liu LX, Zhang WY, et al. Long noncoding RNA MEG3 suppresses epithelial to mesenchymal transition by inhibiting the PSAT1 dependent GSK3beta/Snail signaling pathway in esophageal squamous cell carcinoma. *Oncol Rep.* 2020;44(5):2130–42.
41. Duan W, Liu X. PSAT1 upregulation contributes to cell growth and cisplatin resistance in cervical cancer cells via regulating PI3K/AKT signaling pathway. *Ann Clin Lab Sci.* 2020;50(4):512–8.
42. Sun L, Song L, Wan Q, et al. Cmyc-mediated activation of serine biosynthesis pathway is critical for cancer progression under nutrient deprivation conditions. *Cell Res.* 2015;25(4):429–44.
43. DeNicola GM, Chen PH, Mullarky E, et al. NRF2 regulates serine biosynthesis in non-small cell lung cancer. *Nat Genet.* 2015;47(12):1475–81.
44. Chin AF, Elisseff JH. Senescent cells in tissue engineering. *Curr Opin Biotechnol.* 2022;76:102737.
45. Leyendecker Junior A, Gomes Pinheiro CC, Lazzaretti Fernandes T, et al. The use of human dental pulp stem cells for in vivo bone tissue engineering: a systematic review. *J Tissue Eng.* 2018;9:2041731417752766.
46. Yan S, Jiang H, Fang S, et al. MicroRNA-340 inhibits esophageal cancer cell growth and invasion by targeting phosphoserine aminotransferase 1. *Cell Physiol Biochem.* 2015;37(1):375–86.
47. D'Aniello C, Fico A, Casalino L, et al. A novel autoregulatory loop between the Gcn2-Atf4 pathway and L-proline metabolism controls stem cell identity. *Cell Death Differ.* 2015;22(7):1234.
48. Kim HJ, Yi SW, Oh HJ, et al. Transfection of gene regulation nanoparticles complexed with pDNA and shRNA controls multilineage differentiation of hMSCs. *Biomaterials.* 2018;177:1–13.
49. Yang SY, Wei FL, Hu LH, et al. PERK-eIF2alpha-ATF4 pathway mediated by endoplasmic reticulum stress response is involved in osteodifferentiation of human periodontal ligament cells under cyclic mechanical force. *Cell Signal.* 2016;28(8):880–6.
50. Yao S, Zhao W, Ou Q, et al. MicroRNA-214 suppresses osteogenic differentiation of human periodontal ligament stem cells by targeting ATF4. *Stem Cells Int.* 2017;2017:3028647.
51. Bialopiotrowicz E, Noyszewska-Kania M, Kachamakova-Trojanowska N, et al. Serine biosynthesis pathway supports MYC-miR-494-EZH2 feed-forward circuit necessary to maintain metabolic and epigenetic reprogramming of Burkitt lymphoma cells. *Cancers.* 2020;12(3):580.

Publisher's Note

Springer Nature remains neutral with regard to jurisdictional claims in published maps and institutional affiliations.

Ready to submit your research? Choose BMC and benefit from:

- fast, convenient online submission
- thorough peer review by experienced researchers in your field
- rapid publication on acceptance
- support for research data, including large and complex data types
- gold Open Access which fosters wider collaboration and increased citations
- maximum visibility for your research: over 100M website views per year

At BMC, research is always in progress.

Learn more biomedcentral.com/submissions

